

W. GUMOWSKA*, I. DOBOSZ*, M. UHLEMANN**, J. KOZA**

Al₂O₃ – Co AND Al₂O₃ – Fe COMPOSITES OBTAINED BY THE ELECTROCHEMICAL METHOD

OTRZYMYWANIE KOMPOZYTÓW Al₂O₃ – Co i Al₂O₃ – Fe METODĄ ELEKTROCHEMICZNĄ

The electrochemical method for obtaining the oxide coatings of the Al-Al₂O₃-M composite structure is based on a two-stage process:

- anodic oxidation of aluminium with the formation of a porous oxide coating
- cathodic deposition of 'foreign' metal ions (e.g. Ni, Co, Fe, Cu, Ag, etc.) from an aqueous solution with the direct, pulsating, reversing, or alternating current.

In the present study, the oxide layers on aluminium with an ordered pore structure were obtained in a two-stage process of anodic oxidation in an oxalic acid solution. In the Al₂O₃ layers that are obtained, the cell parameters were changed by pore widening and barrier layer thickness reduction. These processes resulted in obtaining thin membranes, in which cells in the aluminium oxide layer had the following dimensions: pore diameter of ~ 80 nm, single pore wall thickness of ~ 25 nm, and a height of ~ 5 µm. Those membranes were used as a 'templates' for the incorporation of cobalt and iron particles.

The metals were deposited in to membrane pores by the electrodeposition of cobalt and iron from sulphate electrolytes. Measurements were carried out using direct and reversing current (PRC).

The microscopic observations of cobalt and iron nanowires indicate that the membrane pores were not entirely filled by deposited metals. Although in practice, each pore was 'built-up' by a metal, but the length of the nanowires ranged from 1 (Co) to 2 µm (Fe), while the pore height in the membrane was approx. 5 µm.

The cathode efficiencies of the studied metals electrodeposition were determined by using direct current. These efficiencies were not high due to hydrogen co-evolution.

Metoda elektrochemiczna otrzymywania powłok tlenkowych o budowie kompozytowej Al-Al₂O₃-M bazuje na procesie dwuetapowym :

- anodowe utlenianie aluminium z wytworzeniem porowatej powłoki tlenkowej
- katodowa redukcja jonów „obcego” metalu (np.Ni, Co, Fe, Cu, Ag itp.) z zastosowaniem prądu stałego, pulsacyjnego, rewersyjnego lub zmiennego.

W przedstawianej pracy otrzymywano warstewki tlenkowe na aluminium, o uporządkowanej strukturze porów, w dwuetapowym procesie anodowego utleniania w roztworze kwasu szczawowego. W otrzymanych warstewkach Al₂O₃ zmieniano parametry komórek przez poszerzenie porów oraz zmniejszenie grubości warstwy zaporowej. W wyniku tych procesów uzyskano cienkie membrany, w których komórki w warstewce tlenku glinu miały następujące wymiary: średnica porów ~ 80 nm, grubość ścianek ~ 25 nm, a ich wysokość ~ 5 µm. Membrany te stanowiły „szablony” dla wbudowywanych metali : kobaltu i żelaza.

Metale osadzono w porach membrany w procesie katodowej redukcji jonów Co²⁺ i Fe²⁺ z elektrolitów siarczanowych. Pomiary prowadzono z zastosowaniem prądu stałego i rewersyjnego (PRC).

Obserwacje mikroskopowe uzyskanych nanodrutów kobaltu i żelaza wskazują, że w żadnym przypadku pory membrany nie były wypełnione całkowicie przez osadzane metale. Wprawdzie praktycznie każdy por został „zabudowany” przez metal, jednak długość otrzymanych nanodrutów wynosiła od 1 (Co) do 2 µm (Fe), podczas gdy wysokość porów w wytworzonej membranie wynosiła około 5 µm.

Wyznaczono katodowe wydajności prądowe elektroosadzania badanych metali z zastosowaniem prądu stałego. Wydajności te nie są zbyt wysokie ze względu na współwydzielanie wodoru.

* AGH UNIVERSITY OF SCIENCE AND TECHNOLOGY, FACULTY OF NON-FERROUS METALS, 30-059 KRAKÓW, 30. MICKIEWICZA AV., POLAND

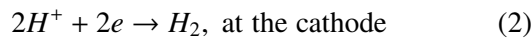
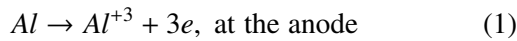
** LEIBNIZ INSTITUT FÜR FESTKÖRPER UND WERKSTOFFFORSCHUNG DRESDEN

1. Introduction

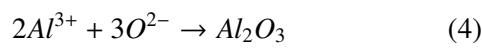
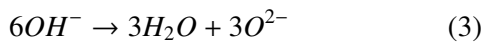
Aluminium is a chemically active metal, with a high affinity to oxygen, and despite that it is still resistant to the corrosive action of numerous environments and a number of chemical reagents. Aluminium shows its resistance due to the protective nature of the oxide layer on the metal's surface. The porous and ordered structure of the oxide layers obtained on aluminium in the process of anodic oxidation is especially appropriate to production of $Al-Al_2O_3-M$ (M – other metal) composite layers.

The oxide layers on aluminium are most often produced in the process of anodic oxidation in the sulphuric, oxalic, phosphoric, or chromic acids solutions [1-11].

The following electrode reactions occur in the process by using a direct current :



The layer of aluminium oxide forms in the reaction of Al^{3+} ions with O^{2-} ions:



- Porous alumina layer forms in consecutive stages:
- formation of a thin (0.01 – 0.1 μm) oxide layer, the so-called blocking or barrier layer
- transformation of the barrier layer on the boundary of phases: oxide – electrolyte (formation of a porous layer)
- increase in the porous layer thickness (from a few to a few dozen μm)

The alumina layer characterizes with ordered structure in the form of hexagonal close-packed ‘honeycomb’ type cells. In each of them are centrally located pores, separated from the metal surface by a thin, so-called barrier layer.

Fig. 1 shows the schematic oxide layer structure (a), ordered cells structure, (b) and the structure and dimensions of a single cell (c).

The pore and cell dimensions as well as the barrier layer thickness are depend on the voltage applied in the process of anodic aluminium oxidation; they also depend on the electrolyte type, composition, and temperature [12-15].

In their studies Keller et al. [12] described in detail the results referring to the relation between individual cells’ dimensions and the anodizing conditions. Composition of electrolytes and process parameters are shown in Table 1.

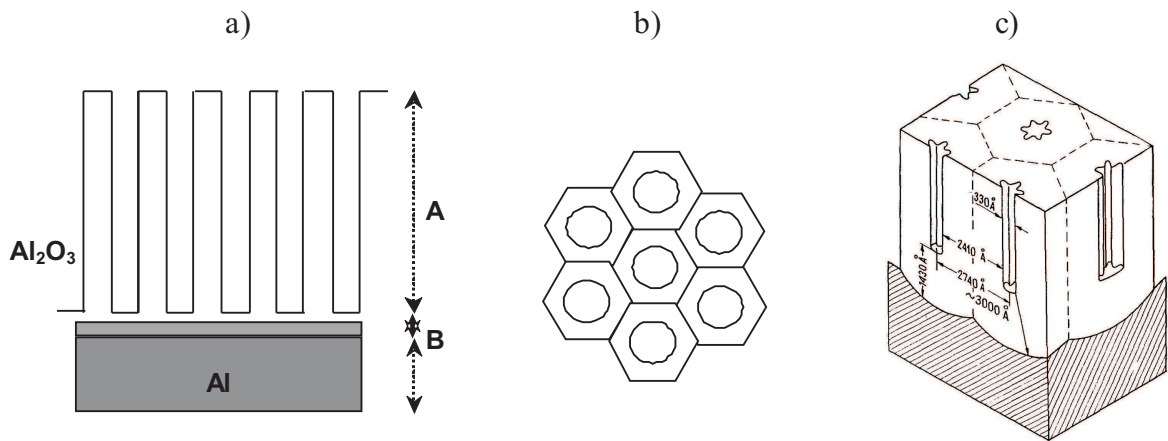


Fig. 1. Diagram of the porous structure of the oxide layer obtained in the process of anodic oxidation of aluminium.

a. A – porous layer, B – barrier layer

b. ordered hexagonal structure of the porous layer

c. structure and dimensions of a single cell of the oxide layer that was obtained in the process of anodic oxidation of aluminium in a 4% solution of phosphoric acid at a voltage of 120 V, [12]

TABLE 1
Conditions of anodic oxidation of aluminium [12]

Electrolyte	Temperature, t°	Electrolysis voltage, U	Cells number, N
	°C	V	$\frac{N \cdot 10^{-9}}{cm^2}$
15% sulphuric acid	10	15	77
		20	52
		30	28
2% oxalic acid	24	20	36
		40	12
		60	6
3% chromic acid	49	20	22
		40	8
		60	4
4% phosphoric acid	24	20	19
		40	8
		60	4

The data in the table show that the cells' (and hence the pores) number changes in a relatively wide range, from $4 \cdot 10^9$ to $77 \cdot 10^9$ (per 1 cm^2 of surface). This depends on the type of electrolyte and on the voltage applied in the process. At the same time, the pores' dimensions were seen to change, namely: the smallest in diameter (120 \AA) pores were obtained in the sulphuric acid solutions, while in phosphoric acids solutions, the pores diameter was the largest, equal to 330 \AA .

Extensive investigations on formation and the methods for creating an appropriately ordered structure of the Al_2O_3 layer [16-21] have increased interest in this system in recent years. Al- Al_2O_3 composite is a material of special applications in the processes of obtaining nanomaterials based on a porous and ordered structure of the oxide layer on aluminium, which works as a template to incorporate specific materials in its pores. In this way the nanowires of metals, metal alloys, or multilayer Al_2O_3 – metal (alloy) composite systems of the reproduced structure of the membrane used are obtained (replica method) [8-12, 16-24].

Thin layers become especially interesting for information technologies (IT) for high – density magnetic recording systems. They are used for production of mini-disks, hard disks, video players and recorders, in personal computers and car navigation systems. Because of the demand for such equipment with increasingly high speed of information recording, the requirements related to the magnetic flux density have been sharply increased. Since 2002 this amount increased from 150 Gbit/inch^2 (23 Gbit/cm^2) to 200 Gbit/inch^2 (31 Gbit/cm^2) and even to 1 Tbit/inch^2 (0.155 Tbit/cm^2) [18].

Magnetic materials for information carriers are based on layers with high magnetic anisotropy in the

perpendicular direction to the layer surface. For the first time a perpendicular system of recording was suggested by Iwasaki [25]. The electrodeposition of cobalt or its alloys' (e.g. CoFe, CoNi, CoNiFe, etc.) nanowires in aluminium oxide pores is most frequently used to obtain magnetic information carriers [19, 20, 26].

The basic stages of the process resulting in the obtaining of nanomaterials in Al_2O_3 layer pores comprise:

- appropriate preparation of an Al_2O_3 matrix in the form of a membrane
- selection of parameters of metal or alloy electrodeposition in the pores.

It has been shown that an oxide layer on aluminium with an high ordered structure forms as a result of two-stage anodising [5, 17, 21, 27, 28]. A detailed description of this method was presented by Nielsch [17].

The first stage of the process consists of a long-lasting (a few dozen hours) anodic oxidation of aluminium at a voltage of 40V, which leads to the typical hexagonal cell structure of aluminium oxide. A 3% solution of oxalic acid is used as the electrolyte at a temperature of 2°C . As the aluminium oxide layer after this process features non-uniform pore distribution, it is chemically removed in a phosphoric acid solution or in a mixture of phosphoric and chromic acids. Once this layer is removed, a hexagonal pore structure remains on the aluminium surface, which is the 'template' for the uniform hexagonal structure of the layer forming in the second stage of anodic oxidation.

The second anodizing stage is relatively short (a few hours) and proceeds in a few steps: anodic oxidation, chemical pore widening, and barrier layer thinning. The dependence of electrolysis voltage and current density on the anodizing time is recorded during this process and some anodizing parameters are gradually changed. Figure 2 shows the schematic course of the consecutive parts of the second anodizing stage (I) and corresponding changes of the oxide layer structure (II). Dotted lines also mark the symbolic stages before (a) and after (e) the second stage of anodic aluminium oxidation to enable a comparison of the differences occurring in the layer structure.

The relationships in the figure 2 show that a minimum of current density is observed at the beginning period of the second stage of anodic oxidation, corresponding to the barrier layer formation. During the continued oxidation, up to an hour approx., the rate of layer formation stabilises (the rate of aluminium oxide formation is equal to the rate of its dissolution by the electrolyte), and as a result the barrier layer thickness stabilises.

Further treatment of the alumina membrane leads to the reduction of the barrier layer thickness. It is carried out by the further oxidation in the same solution at a

temperature of approx. 30°C. Under those conditions, the rate of layer dissolution is higher than the rate of its formation, which leads to pore widening and barrier layer

thinning. The process is accompanied by decreasing electrolysis voltage, which after 4 hours decreases to 25 V.

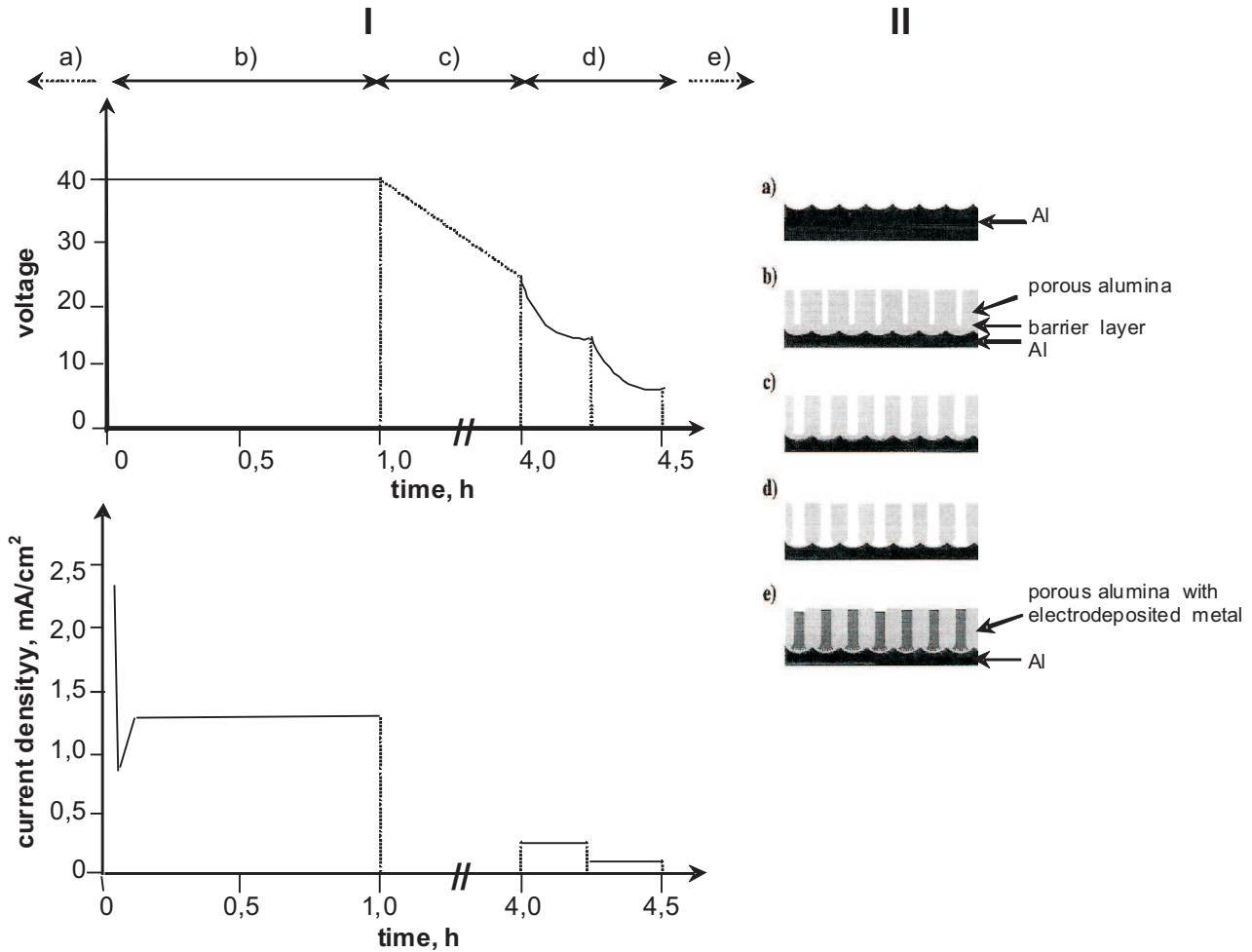


Fig. 2. The course of voltage and current density versus time in the process of anodic oxidation of aluminium (I) and the structure of the layer formed in each of the steps (II) [17]: a. the first anodizing step – long-lasting anodic oxidation in a 3% solution of oxalic acid, at 2°C, and removal of the oxide layer of an unordered structure b. the second anodizing step – obtaining an ordered oxide structure c. pore widening ($t^\circ = 30^\circ\text{C}$) with a simultaneous barrier layer thinning d. further reduction of the barrier layer thickness e. ‘foreign’ metal electrodeposition in membrane pores

The next step consists of breaking the process of pore widening, which is achieved by cooling the electrolyte to 2°C. Then, for further reduction of the barrier layer thickness, lower current densities are used during the anodic oxidation than that at the initial stage.

The final effect of the described preparations of an Al-Al₂O₃ membrane is the reduction of the barrier layer thickness to 10 nm. At the same time, the electrolysis voltage in the studied system reduces to 6-7 V.

Careful preparation of an aluminium oxide matrix guarantees that Al-Al₂O₃-Metal (or alloy) composites featuring a uniform and densely-packed structure are obtained in the process of ‘foreign’ metal electrodeposition

in the oxide layer pores. This process is carried out using direct, alternating, pulsating, or reversing current.

As the application of direct current usually results in non-uniform pore build-up, most of these composites are obtained by using alternating, pulsating or reversing current [17, 22]. During the flow of alternating or reversing current, in cathodic periods of current flow, the incorporation metal ions are reduced according to the reaction:



which is accompanied by hydrogen co-evolution (reaction 2).

The hydrogen co-evolution is an unfavourable process:

- it causes a decrease in the cathodic efficiency of metal electrodeposition
- gaseous hydrogen may block the pores in the layer
- cathodic reduction of hydrogen ions results in a pH increase – electrolyte alkalisation occurs close to the cathode surface, which may cause metal hydroxide precipitation and even damage to the porous ordered structure of the alumina layer.

The application of pulsating or reversing current hinders out those unfavourable effects in the periods of reverse current flow to a large extent.

It should be emphasised that the production of the nanomaterials requires individual techniques, depending on the type of composite. The barrier layer is very often removed, which leads to a structure with pores open on both sides.

The process of gold nanowires, based on an Al_2O_3 membrane, can be used as an example (Fig. 3 [24]).

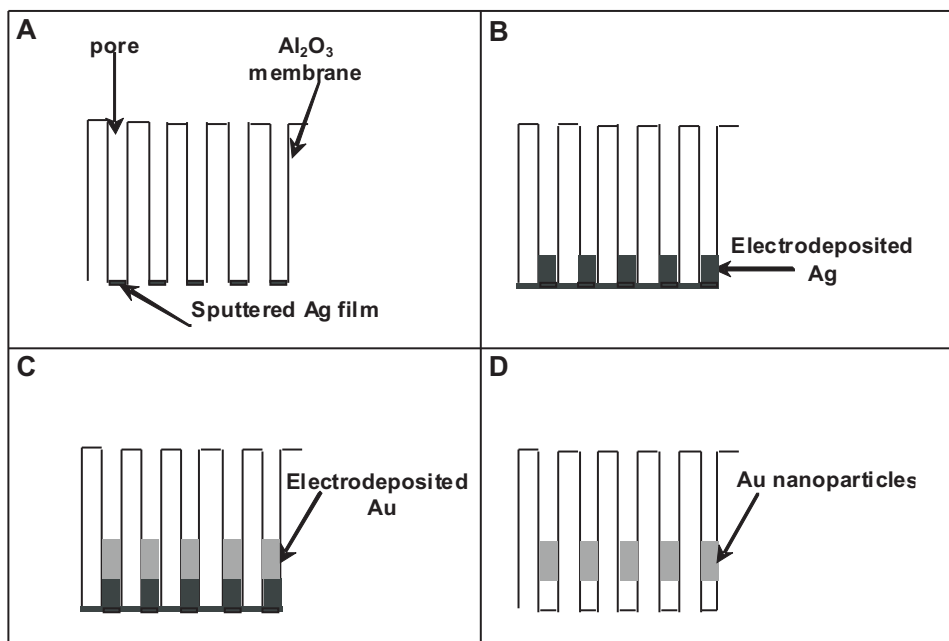


Fig. 3. Diagram of gold nano-wires production

In the first step (A) silver was sputtered on an Al_2O_3 matrix surface and afterwards: silver (B) and then gold (C) were consecutively electrodeposited. The final step was the removal of the silver with nitric acid (D).

Nanocomposites that are based on the ordered structure of an oxide layer on aluminium: Al- Al_2O_3 -Metal (or alloy) and Al_2O_3 -Metal (or alloy) constitute a group of modern materials characterized with special properties and wide range of applications.

In the present study, cobalt and iron nanowires were obtained in the process of those metals electrodeposition in the pores of an alumina membrane on a copper plate.

2. Experimental

2.1. Materials

The specimens were aluminium of the composition: Al – min. 99.999%; Cu – 0.3 ppm; Fe – 0.3 ppm; Mg – 1.2 ppm; Si – 0.8 ppm (Goodfellow).

The specimen's surface was 0.8 cm^2 and 0.3 mm thick. Before the measurements were performed, the specimens were degreased in acetone for 3 minutes, with the application of ultrasound. Then the specimens were annealed in an argon atmosphere for 3 hours, at 500°C , to remove any residual stress and for homogenization of its composition.

The annealed specimens were electropolished (Stuers LectroPol-5 electropolisher) in a mixture of HClO_4 and $\text{C}_2\text{H}_5\text{OH}$ solutions with the addition of butyl cellulose. Table 3 shows the parameters of electropolishing.

Parameters of electropolishing

Temperature	16°C
Time	20 s
Voltage	48 V
Electrolyte flow	16 cm ³ /min
Electrolyte composition	78 cm ³ HClO ₄ 700 cm ³ C ₂ H ₅ OH 100 cm ³ butyl cellulose 120 cm ³ H ₂ O

2.2. Anodic oxidation of aluminium

The anodic oxidation process was carried out in two steps. 0.3 M oxalic acid was used in both of them. The first step was carried out at constant electrolysis voltage

TABLE 2

of 40V and 2°C. Low temperature is needed during anodizing steps because temperatures higher than 5°C may cause thermal shocks and breakdowns in the barrier layer [17].

The schematic diagram of the experimental apparatus is shown in Fig. 4.

The electrolyser (made of Teflon) had an opening in the bottom, in which the Al anode was fixed. One surface of the specimen was in contact with the electrolyte, the other – external – with a copper plate, which ensured the current connection to the aluminium electrode. The cathode was made of aluminium and placed parallel to the specimen. To ensure low temperatures, the system was cooled using a cryostat. Temperature of electrolyte was measured continuously. The electrolyte was stirred by means of a mechanical stirrer.

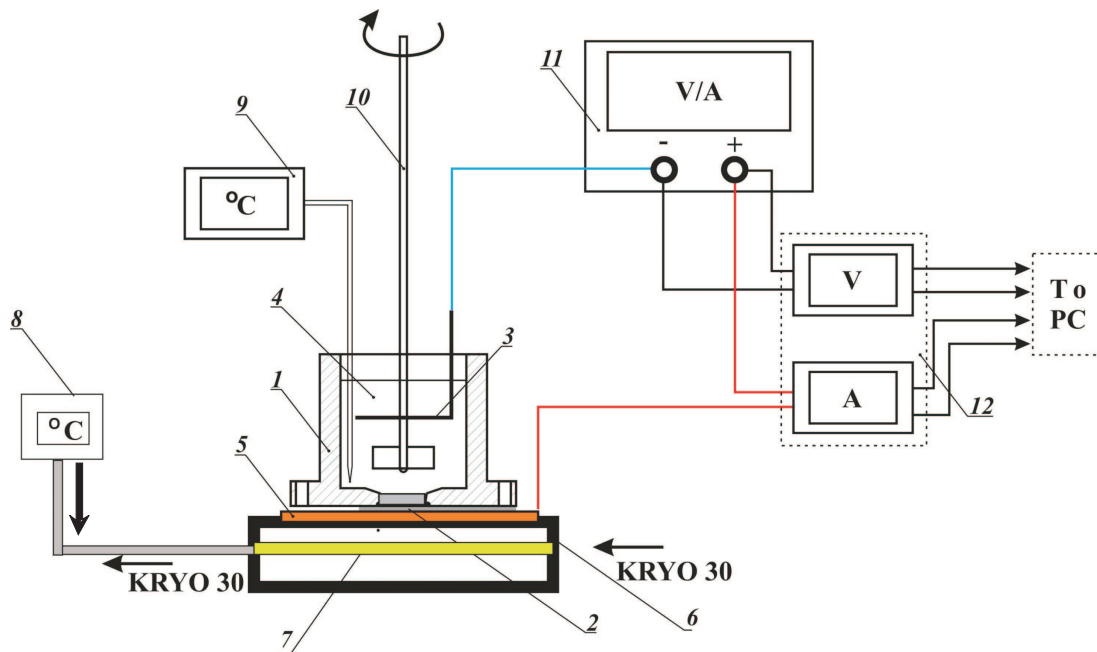


Fig. 4. Diagram of the experimental set. 1 – electrolyser, 2 – Al anode, 3 – Al cathode, 4 – electrolyte, 5 – Cu block, 6 – aluminium block, 7 – pipe with KRYO 30 cooling liquid, 8 – cryostat, 9 – temperature controller, 10 – stirrer, 11 – stabilised power supply, 12 – data recording system (KEITLEY 199)

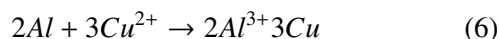
The time of the first anodising step was 24 hours. The oxide layer that was obtained in this step was removed in a solution containing H₃PO₄ (35 cm³/dm³) and CrO₃ (20g/dm³) at 80°C for 2 hours. After the oxide layer removal, the specimens were anodic oxidised (step two) for 5 hours. Then the specimens were subjected to pore widening by heating the oxalic acid up to 40°C for 2 hours. In the next step, which aimed at the thinning of the barrier layer, the anodizing was continued, during which the electrolysis voltage was gradually reduced from 10.1 to 5.0 V. These parameters are shown in Table 3.

TABLE 3
Parameters of the thinning process of the barrier layer

Anodizing voltage, V	Time, min
10.1	3
8.8	3
7.5	3
6.9	3
5.0	3

2.3. Aluminium and barrier layer removal

The aluminium substrate was dissolved after two anodizing steps. This process was carried out in a 1:3 mixture of HCl and CuCl₂ solutions (100 cm³ of 38% HCl + 3,4 g of CuCl₂·H₂O + 100 cm³ H₂O), at room temperature for approx. 45-60 minutes. In these conditions the aluminium react with CuCl₂ solution:



After this process, the pores opened. The barrier layer was etched in a 5% H₃PO₄ solution at 30°C for 15 minutes.

2.4. Substrate deposition

After removal of the aluminium and barrier layer, a thin layer of gold was sputter on the fracture of the template (on the open pores of the external specimen's surface). Then, copper was electrolytically deposited from a sulphate bath. The composition of electrolyte was: 65g CuSO₄, 184g H₂SO₄ and 105 mg KCl in dm³. The electrolysis was carried out using direct current, under potentiostatic conditions at potential -300 mV (vs SCE); the time of electrolysis – 10 minutes. IPS AJ potentiostat was used in the measurements.

In this way the porous membranes were obtained with the structure, which is shown in the diagram in Fig. 5.

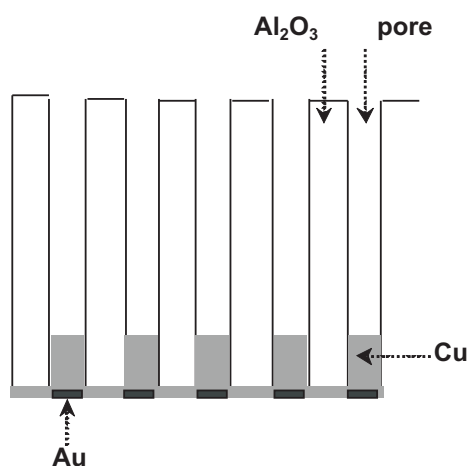


Fig. 5. Diagram of the alumina membrane structure

Sputtering gold is aimed at the closing pores, while the layer of electrodeposited copper causes a reduction of electrolysis voltage in the process of metal electrodeposition in the pores of an Al₂O₃ layer.

2.5. Cathodic deposition of metals

The process of cobalt and iron incorporation in to the membrane pores was carried out in the electrodeposition of Co²⁺ and Fe²⁺ ions from sulphate baths, applying direct or reversing current (PRC). Electrodeposition was carried out using IPS AJ potentiostat at room temperature. The composition of electrolytes is shown in Table 4.

TABLE 4
Composition of electrolytes for Co and Fe deposition

Electrolysis	Electrolyte composition	pH
Cobalt deposition	140.6 g/dm ³ CoSO ₄ ·7H ₂ O 25 g/dm ³ H ₃ BO ₃	3.0
Iron deposition	139 g/dm ³ FeSO ₄ ·7H ₂ O 25 g/dm ³ H ₃ BO ₃	2.6

In the process of metal electrodeposition, the specimen (membrane) was placed horizontally in the electrolyser made of Teflon. A platinum sheet was an auxiliary electrode, while the saturated calomel electrode was the reference electrode.

Analytical purity reagents were used to prepare the solutions. The pH value was controlled by the addition of a 10% H₂SO₄ or NaOH solution.

Electrodeposition was carried out using direct current, under potentiostatic conditions (E = -1.2 V (vs. SCE)), or by using reversing current (PRC). IPS AJ potentiostat was used in the measurements.

The measurements under PRC conditions were performed by applying:

the time of cathodic current flow t_K = 140 ms; potential E_K = -1.2 V (vs. SCE);

the time of anodic direction of the current flow t_A = 20 ms; potentials:

E_A = 0 V (vs. SCE) for Co; E_A = -0,350 V (vs. SCE) for Fe.

Selected materials were subjected to observations on a scanning electron microscope (FE Gemini LEO 1530).

3. Results and discussion

3.1. Membrane preparation

Membrane preparation is an important step in the nanowire deposition. Depending on the anodizing parameters (voltage, time) applied, we can control the pore diameter and height.

During step I of anodic oxidation of aluminium, the relationship between current and time was recorded. The course of such a relationship is shown in Figure 6.

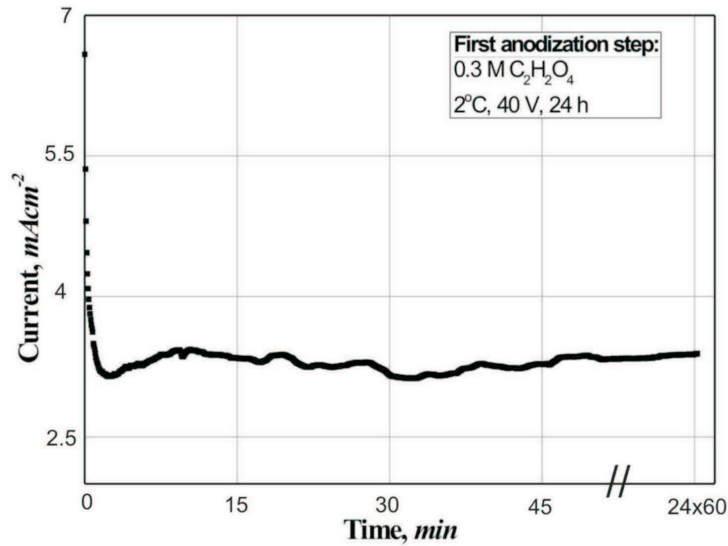


Fig. 6. Current density versus time during the first step of anodizing

A sudden decrease in the current intensity was observed in the initial stage of the process, which is related to the beginning of the oxide barrier layer formation. After a few minutes, the rate of the layer formation is equalised with the rate of its dissolution by the electrolyte – a constant current intensity is observed.

Pores start growing in various directions and pores distribution in the oxide is entirely irregular. Therefore, after a long-lasting period of the first anodising step

the porous unordered oxide structure was removed in a solution containing H_3PO_4 ($35\text{ cm}^3/\text{dm}^3$) and CrO_3 ($20\text{g}/\text{dm}^3$) at 80°C for 2 hours. Cavities remain after oxide removal, which make the template for future pores formation. After this process, the specimen was subjected to repeated anodic oxidation (step II). Fig. 7 shows the dependence of the anodic current density on oxidation time.

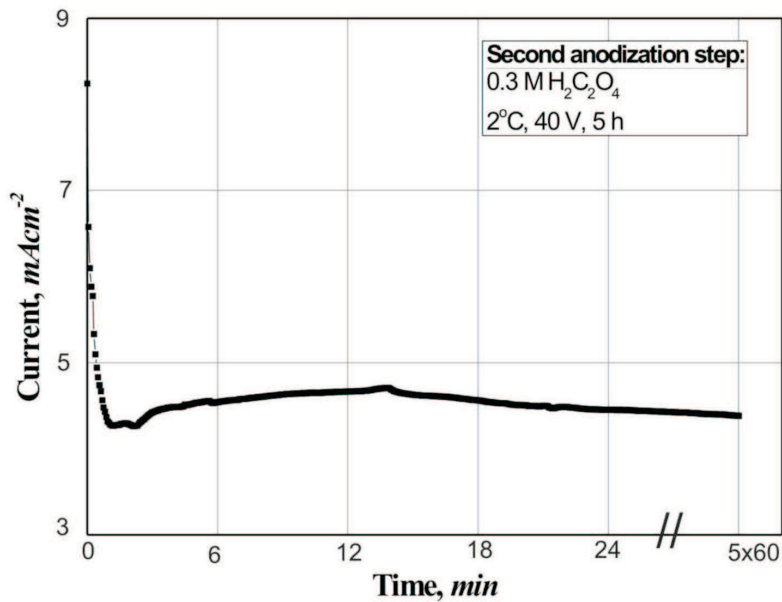


Fig. 7. Current density versus time during the second step of anodizing

As a result of the second anodizing step, the pores grow perpendicular to the surface and form an ordered

hexagonal structure, which was confirmed by scanning microscope observations (Fig. 8).

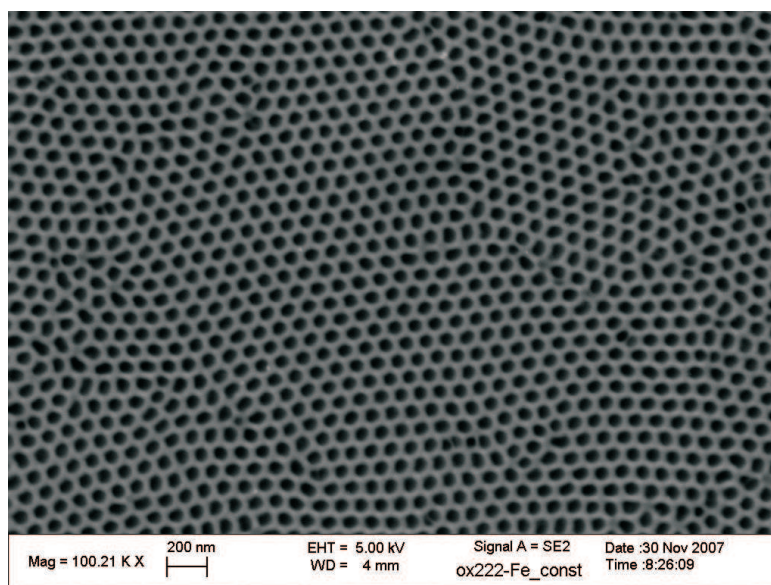


Fig. 8. Microstructure of aluminium specimen after the second anodizing stage

Pore dimensions and the porosity of the membrane are shown in Table 5.

Dimensions of membrane obtained

TABLE 5

Pore diameter	Pore height	Distance between the pores	Surface fraction of pores
D_p <i>nm</i>	L μm	l <i>nm</i>	%
~ 80 ($\sim 0,08 \mu m$)	~ 5	~ 105 ($\sim 0,1 \mu m$)	~ 50

3.2. Nanowire deposition

Cobalt and iron nanowires were obtained in the process of electrodeposition in the nanopores of an aluminium oxide membrane under potentiostatic conditions by using direct or reversing (PRC) current.

3.2.1. Electrodeposition of cobalt nanowires – direct current

Cobalt was deposited from sulphate baths of the composition shown in Table 4. Cyclic voltammetry was

applied to determine the optimal potentials for Co electrodeposition.

The dependence of current density on potential $i = f(E)$ is obtained from cyclic voltammetry. This relationship is shown in Figure 9. The potentials are given versus SCE.

Based on voltammogramme, it is possible to conclude that cobalt electrodeposition occurs in the potentials that range from -0.7 V to -1.2 V.

A potential was selected from this range, at which cobalt was electrodeposited in membrane pores, based on the values of cathodic current efficiency.

Cathodic current efficiencies were determined from an electrode mass increase, in which the amount of charges flowing through the system was determined by planimetry of $I = f(t)$ curve. The measurement was performed at a few potentials, which values result from the voltammetry. The relationship between the current efficiency and potential is shown in Figure 10.

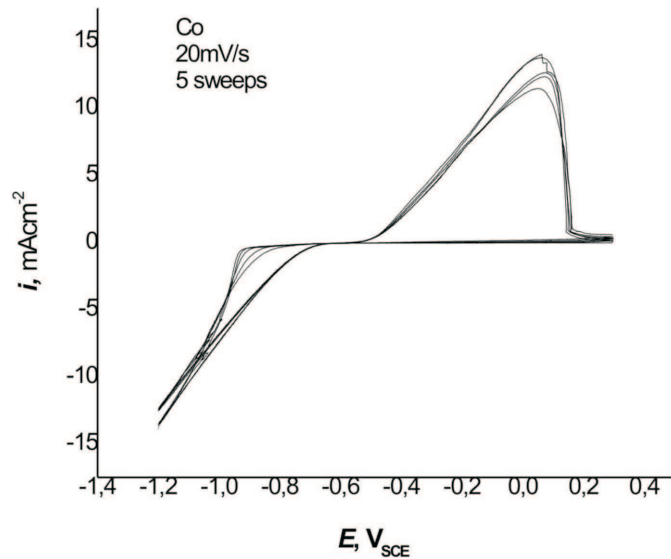


Fig. 9. Voltammogramme for cobalt

The maximum of cathodic efficiency was observed at the potential of -1.2 V . This potential was selected as the most appropriate in the measurements of cobalt

electrodeposition, because it ensures the highest degree of metal incorporation into the membrane pores.

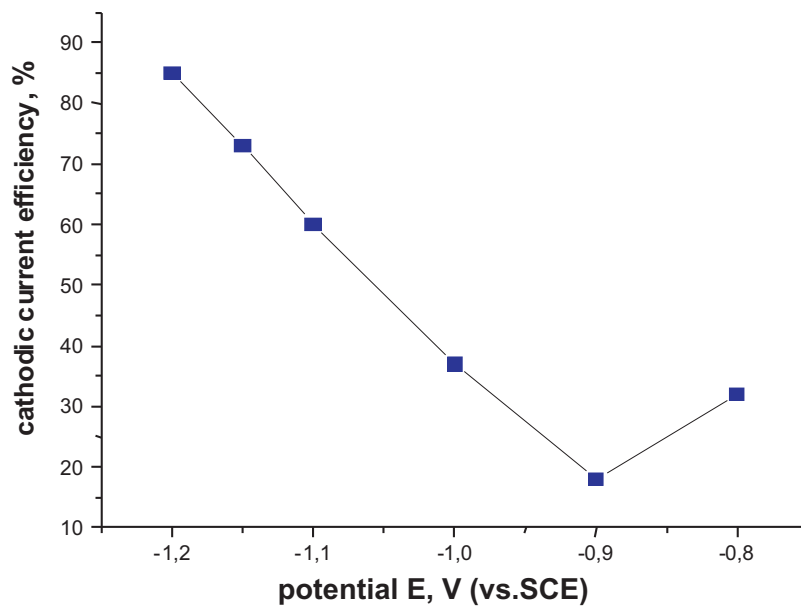


Fig. 10. Dependence of cathodic current efficiency on the potential cobalt electrodeposition

Specimens after cobalt electrodeposition were observed on a scanning microscope. The pore diameter and nanowire height was determined. Observations of the cross-section of the Al₂O₃ – Co were carried out. Fig.

11 shows the microphotograph of Co nanowires obtained during electrodeposition in potentiostatic conditions, (E = -1.2 V(vs. SCE)).

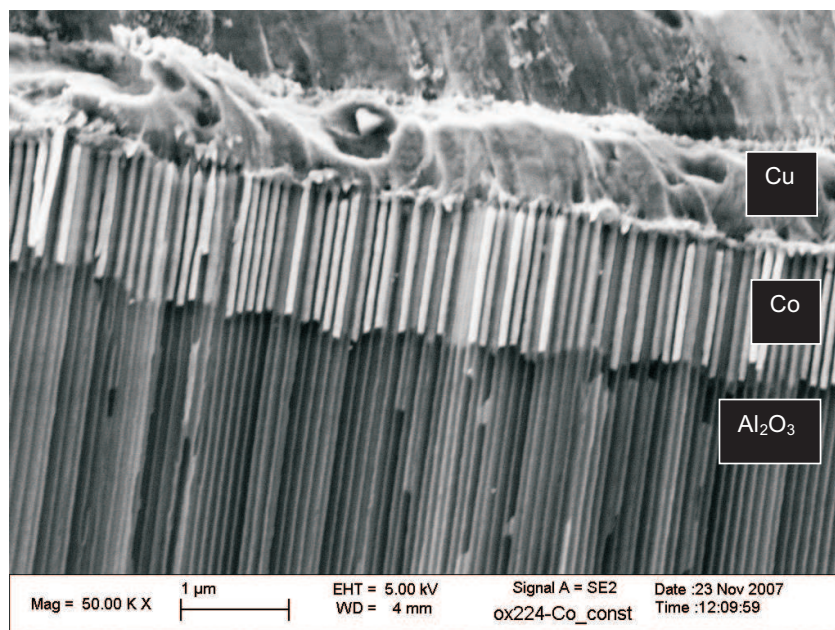


Fig. 11. SEM images of template after Co electrodeposition under direct current, $E = -1.2$ V (vs.SCE)

The obtained nanowires are uniform, cobalt is deposited in each pore and the pores are around $1 \mu\text{m}$ high.

On the composite surface, on Al_2O_3 – electrolyte phase boundary, a deposit of cobalt hydroxide was observed (in the picture – below Al_2O_3), which is not seen in the microphotograph presented. It is formed due to the pH decrease resulting from the cathodic reduction of hydrogen ions (reaction (2)).

3.2.2. Electrodeposition of cobalt nanowires – reversing current (PRC)

Cobalt was deposited from sulphate baths of the composition shown in Table 4. Reversing current of the

following parameters was used in the process of electrodeposition: $E_K = -1.2$ V (vs. SCE), $t_K = 140$ ms; $E_A = 0$ V (vs.SCE), $t_A = 20$ ms.

Specimens were subjected to observations on a scanning microscope. The pore diameter and nanowire height were determined. Observations of the cross-section of the surface were carried out. Fig. 12 shows the microphotograph of Co nanowires obtained during electrodeposition under PRC conditions.

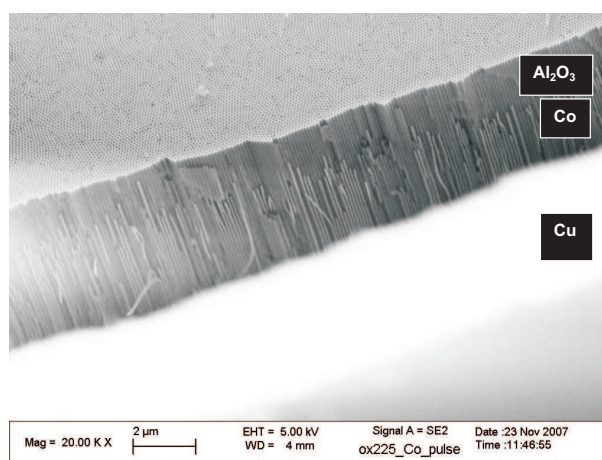


Fig. 12. SEM images of template after Co electrodeposition using reversing current: $E_K = -1.2$ V (vs. SCE), $t_K = 140$ ms; $E_A = 0$ V (vs. SCE) $t_A = 20$ ms

The nanowires are not uniform and differ in height. Cobalt is deposited nearly in each pore.

3.2.3. Electrodeposition of iron nanowires – direct current

Iron was deposited from sulphate baths of the composition shown in Table 4. Cyclic voltammetry was car-

ried out to determine the optimal potentials for Fe electrodeposition. The relationship between the current density and potential $i = f(E)$ is shown in Figure 13.

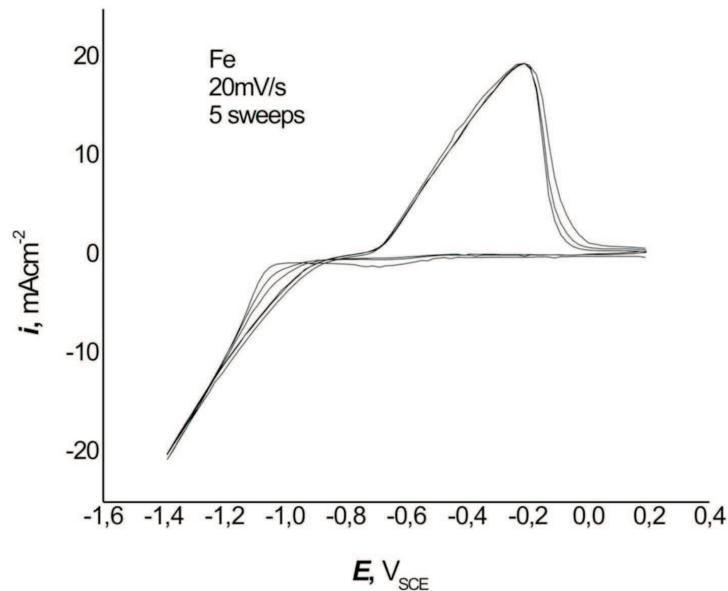


Fig. 13. Voltammogramme for iron

Based on voltammogramme it is possible to conclude that iron electrodeposition occurs in the potentials that range from -0.9 V to -1.4 V.

A potential was selected from this range, at which iron was electrodeposited in the membrane pores, based on the values of cathodic efficiency.

The dependence of cathodic current efficiency on the potential of cathodic Fe^{2+} ions reduction is shown

in Fig. 14. A maximum of cathodic current efficiency is observed at the potential of -1.25 V.

The cathodic current efficiencies, both for iron and cobalt electrodeposition, are not high. This is understandable, because gaseous hydrogen co-evolves apart from metal ions reduction in the cathodic process.

Iron electrodeposition measurements were made at the potential of -1.2 V (vs.SCE).

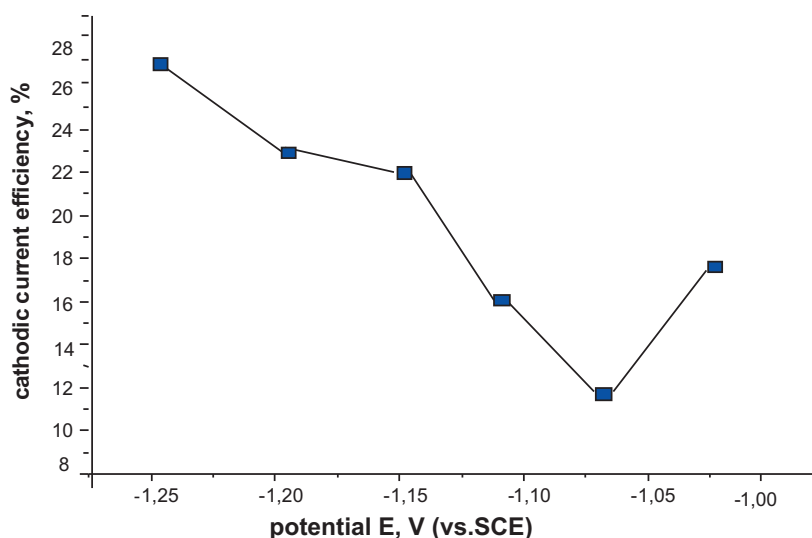


Fig. 14. Dependence of cathodic current efficiency on the potential – iron electrodeposition

Specimens after iron electrodeposition were subjected to observations on a scanning microscope. The pore diameter and nanowire height were determined. Observations of the cross-section of the surface were carried

out. Fig. 15 shows of a microphotograph of the Fe nanowires obtained during direct current electrodeposition under potentiostatic conditions ($E = -1.2$ V (vs.SCE)).

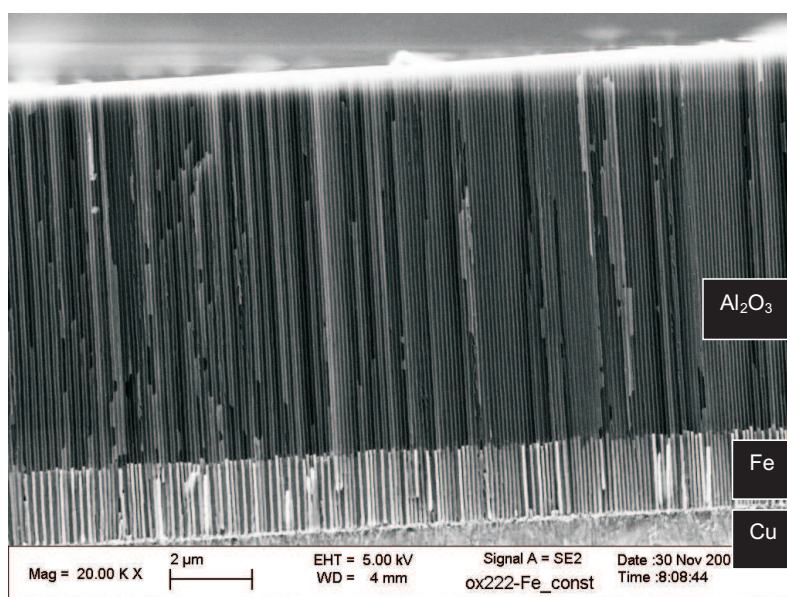


Fig. 15. SEM images of template after Co electrodeposition under direct current, $E_K = -1.2$ V (vs.SCE)

Iron was uniformly deposited in each pore. The nanowires obtained have the same height, equal to approx. 2 μm .

3.2.4. Electrodeposition of iron nanowires – reversing current (PRC)

Iron was deposited from sulphate baths of the composition shown in Table 4. Reversing current of the following parameters was used in the process of electrode-

position: $E_K = -1.2$ V (vs. SCE), $t_K = 140$ ms; $E_A = -0.350$ V (vs. SCE), $t_A = 20$ ms.

Specimens were subjected to observations on a scanning microscope. The pore diameter and nanowire height were determined. Observations of the cross-section of the surface were carried out. Fig. 16 shows a microphotograph of the Fe nanowires obtained during electrodeposition under the reversing current conditions.

The microphotograph shows that iron is deposited in each pore. The nanowires are not uniform and differ in height.

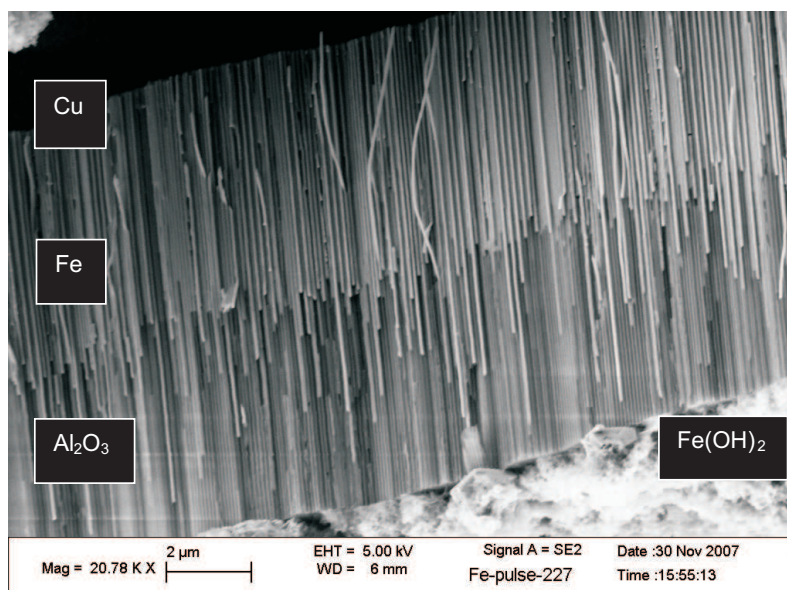


Fig. 16. SEM images of template after Co electrodeposition using reversing (PRC) current: $E_K = -1.2$ V(vs.SCE), $t_K = 140$ ms; $E_A = -0.350$ V(vs.SCE) $t_A = 20$ ms

Microscopic observations of the cobalt and iron nanowires (Fig. 11, 12, 15 and 16) indicate that the membrane pores were not entirely filled by deposited metals. Although in practice each pore was fulfilled with a metal, but the length of nanowires ranged from 1 to 2 μm , while the pore height in the membrane amounted to approx. 5 μm .

In the microphotograph, in the Al_2O_3 – electrolyte interface, a clear iron hydroxide deposit is seen, which forms due to a pH decrease as a result of cathodic reduction of hydrogen ions (reaction (2)).

4. Conclusions

1. Nanocomposite Al_2O_3 – Co and Al_2O_3 – Fe were obtained on a copper plate.
2. Cobalt and iron nanowires were obtained in the process of cathodic deposition of those metals ions in the pores of an aluminium oxide layer (membrane). Experiments were performed using direct or reversing (PRC) current.
3. The nanowires distribution in the pores of an aluminium oxide layer is uniform, in the processes of electrolysis using both direct and reversing current.
4. Cathodic efficiencies depend on the potential at which Co and Fe were electrodeposited. The maximum values were obtained during the process carried out at the potential of -1.2 V (vs. SCE). They amount to: 85% for cobalt, 27% for iron. Hydrogen co-evolution is the reason for the relatively low current efficiencies.

Acknowledgements

This research work has been supported by the Polish Ministry of Science and Higher Education under project No. 10.10.180.307.

REFERENCES

- [1] D. Al. Mawlawi, N. Coombs, M. Moskovits, *J.Appl.Phys.* **70**, 70 (1991).
- [2] F. Li, R. M. Metzger, W. D. Doyle, *IEEE Trans. Magn.* **33**, 375 (1947).
- [3] J. Li, M. Moskovits, T. L. Haslet, *Chem.Mater* **10**, 1963 (1998).
- [4] J. S. Suh, J. S. Lee, *Appl.Phys.Lett.* **75**, 2047 (1999).
- [5] J. Jasensky, F. Müller, U. Gösele, *J.Electrochem.Soc.* **145**, (11), 3735 (1998).
- [6] H. Asoh, K. Nishio, M. Nakao, T. Takamura, H. Masuda, *J.Electrochem.Soc.* **148**, (4), B 152 (2001).
- [7] H. Masuda, F. Hasegawa, *J.Electrochem.Soc.* **144**, (5), L 127 (1997).
- [8] G. Sulka, S. Stroobants, V. Moshehalkov, G. Borghs, J.-P. Celis, *J. Electrochem. Soc.* **149**, (7), D 97 (2002).
- [9] G. Sulka, S. Stroobants, V. Moshehalkov, G. Borghs, J.-P. Celis, *J.Electrochem. Soc.* **151**, (5), B 260 (2004).
- [10] G. Sulka, K. G. Parkoła, *Thin Solid Films* **515**, 338 (2006).
- [11] G. Sulka, K. G. Parkoła, *Electrochimica Acta* **52**, 188 (2007).
- [12] F. Keller, M. S. Hunter, D. L. Robinson, *J.Electrochem.Soc.* **100**, 411 (1953).

- [13] A. P. Li, F. Müller, A. Birner, K. Nielsch, U. Gösele, *J.Appl.Phys.* **84**, 6023 (1998).
- [14] R. C. Furneaux, W. R. Rigby, A. P. Davidson, *Nature* **337**, 147 (1989).
- [15] A. Jagminas, D. Bigelienė, J. Mikulskas, R. Tomasiūnas, *J.Crystal Growth* **233**, 591 (2001).
- [16] M. J. Tirney, Ch. R. Martin, *J.Electrochem.Soc.* **137** (12), 3789 (1990).
- [17] K. Nielsch, F. Müller, A. P. Li, U. Gösele, *Adv. Mater.* **12** (8), 582 (2000).
- [18] T. Osaka, T. Asahi, J. Kawaji, T. Yokoshima, *Electrochimica Acta* **50**, 4576 (2005).
- [19] D. H. Qin, L. Cao, Q. Y. Sun, Y. Huang, H. L. Li, *Chem.Phys.Latters* **358**, 484 (2002).
- [20] S. Kawai, R. Meda, *J.Electrochem.Soc.* **122** (1), 32 (1975).
- [21] H. Masuda, K. Fukuda, *Science* **268**, 1466 (1995).
- [22] R. Inguanta, M. Butera, C. Sunseri, S. Piazza, *Appl. Surf. Science* **253**, 5447 (2007).
- [23] A. Jagminienė, G. Valinčius, A. Riaukaitė, A. Jagminas, *J.Crystal Growth* **274**, 622 (2005).
- [24] J. C. Hulten, Ch. R. Martin, *J.Mater.Chem.* **7** (7), 1075 (1997).
- [25] S. Iwasaki, Y. Nakamura, *IEEE Trans. Magn. MAG* **13**, 1272 (1977), w/g [18].
- [26] T. Osaka, N. Nagasaka, F. Goto, *J.Electrochem. Soc.* **128**, 1686 (1981).
- [27] H. Masuda, M. Satoh, *Jpn.J.Appl.Phys.* **35**, L 126 (1996).
- [28] D. G. W. Goad, M. Moskovits, *J. Appl. Phys.* **49**, 2929 (1978).

Received: 10 February 2009.

